

Anomalous inland influx of the River Indus, Gulf of Kachchh, India

Onkar S. Chauhan^a, S. Jayakumar^a, A.A.A. Menezes^a, A.S. Rajawat^b and S.R. Nayak^b

^a National Institute of Oceanography, Dona Paula, Goa, 403 004 India

^b Space Application Center, P.O. SAC Ahmedabad, 380015 India

Abstract

The Gulf of Kachchh is a funnel shaped, macrotidal water body located in the arid region of northwestern India with ~ 50 cm annual rainfall and insignificant fluvial input. The Gulf waters, however, have high-suspended matter. Time series measurements of total suspended matter (TSM) and synchronous, validated hydrodynamic modeling have been used to decipher the dispersal pathways and the sources of the high turbidity. Contrary to the prevalent offshore reducing trend for most of the Indian Coast, the Gulf is anomalous for having an enhanced turbidity at the mouth with lower concentrations in the inland areas. The hydrography of the Gulf is dominated by strong, alongshore currents at the mouth which move in (out) during flood (ebb), and undergo cyclic, dynamic changes with tidal phases. The flood tidal currents amplify inland with propagating tides, pulling in the offshore waters and acting as a feeder of high saline, turbid offshore waters into the Gulf, most of which are trapped inland due to time lag of ebb and flood between the outer and the inner Gulf. Based upon the distribution maps of TSM and clays in the water column, it is deduced that a large segment of the Gulf is nourished by contributions from the Indus River.

1.0 Introduction

Estimated influx of suspended matter world over is about 1.3×10^9 tons. (Milliman and Meade, 1983). Being a measure of turbidity, which regulates penetration of sunlight into the water column, survival of coral reefs and mangrove ecosystems depends on it. All coastal engineering and shore development strategies need accurate determination of drift rates and their dynamics. Normally, for a large fluvial source such as the River Indus (discharging 200 million tons of sediments annually; Nair et al., 1982), it is thought that most of the fluvial discharge is either distributed alongshore or advected into the deeper offshore waters. The amount of terrigenous matter, therefore, in time series sediment traps or in cores, has been linearly correlated with the magnitude of flux of the Indus (Nair et al., 1989; von Rad et al., 1999) along the northern region of the Arabian Sea.

The Gulf of Kachchh ($68^{\circ} 20' - 70^{\circ} 40' E$ and $22^{\circ} 15' - 23^{\circ} 40' N$), a funnel shaped, east – west oriented, macrotidal, seismically active indentation, is one of the three macrotidal regions of India (Fig. 1). It occupies about 7350 km² area. The tides at the mouth of the Gulf are about 4m, which amplify to 7 m in the intricate creeks due to depth and width factors (Chauhan and Vora, 1990). The Gulf is located in a semi-arid region (annual rainfall 50 cm). The Gulf waters, unlike most other estuaries of the west coast of India (which show seasonal stratification), due to prevalent climate and reduced fluvial discharge, have homogeneous one layered structure (Pradhan et al., 2004). The Gulf was subareally exposed prior to Holocene, because the known sea level was about

-65 m prior to 10 Ka BP in this region (Nigam et al., 1992). Past studies have documented a layered, 18 m thick deposition in the Gulf (Chauhan and Vora, 1990). Because the Gulf lies in semi-arid region, and the local fluvial sources are small and estuarine with insignificant sediment discharge, the specific issue, which remains unresolved is the sources of this massive sedimentation during the Holocene under the high-energy macrotidal environment.

The present study has a multidisciplinary approach to determine source to sink pathways in this complex and unique system, and relies on tide phase synchronous measurements of total suspended matter (TSM) and clay minerals in the water column. The synoptic view of the regional distribution of TSM has been obtained from satellite imageries. The results of synchronous hydrodynamic modeling, validated by in situ current measurements for the period of modeling are integrated with TSM measurements to decipher the specific processes that contribute to the anomalous terrigenous flux into the Gulf.

Methodology

Between the inner shelf - inland regions of the Gulf, 26 stations were monitored during high tide (HT), low tide (LT) and mid tide (MT; random tide) during 3 -19 September of 1999, the period during which the southwest monsoon, the main source of rainfall in this region, is prevalent. Conventionally, one liter of water was filtered and the matter retained on $<0.45 \mu\text{m}$ optipure fiber filter paper was considered as TSM. In the present study, we have, in addition to this conventional method, separated terrigenous matter through a 6

feet Prep/Scale TFF regenerated cellulose cartridge (No CDUF 006 Lm) on a tangential flow filtration system of Millipore, which separates $\sim 0.02 \mu\text{m}$ size particulate matter from seawater. About 100 liters of seawater were filtered for each station for acquiring TSM. Because the Gulf is tide dominated and the sediment dynamics are expected to vary with the magnitude of the tide, TSM measurements were carried out twice at each station synchronously during LT, HT and MT conditions, 2 m below the water surface (total samples 156). The currents were measured 2 m below sea surface, at 30 min intervals, using CONtrol Ocean current meter (accuracy of $\pm 5^\circ$ and 2% for direction and magnitude respectively). For validation purpose synchronous current measurements at two locations in the outer and inner regions of the Gulf, 2 m below water surface, at 30 min intervals were carried out during 3-13 September of 1999. The Global Positioning System (GPS) was used for determining the geographical location of each station.

For clay minerals analysis, a fraction of the separated matter was passed through a membrane filter of $\sim 2 \mu\text{m}$. The clays retained on filter paper were dispersed on a glass slide, and air-dried to obtain an oriented sample. Carroll (1970) has suggested treatment with ethylene glycol (glycolation) for expandable clays at 60°C for 1 hour. Considering the small amount of samples, we have glycolated our samples at 100°C for 2 h to resolve duplet of chlorite and smectite. Glycolated samples were analyzed on a X-Ray diffractometer (model: Phillips 1840) using Ni filtered Cu $K\alpha$ radiation ($\lambda = 1.541\text{\AA}$). Clay minerals were identified using the methods of Biscaye (1965). Semi-

quantitative analysis of the clays is done from weighted peak area methods (Biscaye, 1965; Carroll, 1970). The replicate analyses suggest that the results have $\pm 8\%$ precision for smectite and $\pm 5\%$ for the remaining clays.

The hydrodynamic simulation was carried out using MIKE-21 software of the DHI Water & Environment, Denmark, which calculates the flow field from the solution of the depth-integrated continuity and momentum equations (Abbott et al., 1973; Abbott 1979). The vertically integrated equations of conservation of volume and momentum in x and y directions used in the model are:

X-momentum:

$$\frac{\partial p}{\partial t} + \frac{\partial}{\partial x} \left(\frac{p^2}{h} \right) + \frac{\partial}{\partial y} \left(\frac{pq}{h} \right) + gh \frac{\partial \zeta}{\partial x} + \frac{g \sqrt{\frac{p^2}{h^2} + \frac{q^2}{h^2}} p}{C^2} - fVV_x - \frac{h}{p_w} \frac{\partial p_a}{\partial x} - \Omega q - E \left(\frac{\partial^2 p}{\partial x^2} + \frac{\partial^2 q}{\partial y^2} \right) = S_{ix}$$

Y-momentum:

$$\frac{\partial q}{\partial t} + \frac{\partial}{\partial y} \left(\frac{q^2}{h} \right) + \frac{\partial}{\partial x} \left(\frac{pq}{h} \right) + gh \frac{\partial \zeta}{\partial y} + \frac{g \sqrt{\frac{p^2}{h^2} + \frac{q^2}{h^2}} q}{C^2} - fVV_y - \frac{h}{p_w} \frac{\partial p_a}{\partial y} - \Omega p - E \left(\frac{\partial^2 p}{\partial x^2} + \frac{\partial^2 q}{\partial y^2} \right) = S_{iy}$$

Continuity:

$$\frac{\partial \zeta}{\partial t} + \frac{\partial p}{\partial x} + \frac{\partial q}{\partial y} = S - e$$

where x, y are the two spatial coordinates, t is the time, ζ is the water surface level above datum, p is flux density in the x-direction, q is flux density in the y-direction, h is the water depth, S is the source magnitude, S_{ix} , S_{iy} are

source impulse in x- and y- directions respectively, e is evaporation rate, g is acceleration due to gravity, C is Chezy resistance number, f is wind friction factor, V , V_x , V_y are wind speed, wind velocity components respectively, p_a is barometric pressure, ρ_w is the density of water, Ω is the Coriolis force, and E is eddy viscosity coefficient.

The eddy viscosity coefficient, E is expressed as a time-varying function of the local gradients of the velocity field, known as Smagorinsky scheme:

$$E = C_s^2 \Delta^2 \left[\left(\frac{\partial u}{\partial x} \right)^2 + \frac{1}{2} \left(\frac{\partial u}{\partial y} + \frac{\partial v}{\partial x} \right)^2 + \left(\frac{\partial v}{\partial y} \right)^2 \right]$$

where u , v are depth-averaged velocity components in the x and y direction and Δ is the grid spacing. In the present study the velocity-based Smagorinsky scheme with a constant value of $C_s = 0.5$ has been applied for all simulations. The criteria used for eddy viscosity is

$$\frac{E \cdot \Delta t}{\Delta x^2} \leq \frac{1}{2}$$

The bed resistance F is expressed as

$$F = \frac{g \cdot u \cdot |u|}{C^2}$$

where, C is the Chezy number and M is Manning number which is expressed as.

$$C = M \cdot h^{\frac{1}{6}}$$

The dynamic stability of the model is defined using the Courant-Friedrichs-Lewy (CFL) stability criterion:

$$C_R = c \frac{\Delta t}{\Delta x}$$

where, wave celerity $c = \sqrt{gh}$

A model domain 78 km (horizontal) x 46 km (vertical) that covers the entire Gulf of Kachchh has been considered. Simulations were carried out over a period of 30 days during September 1999 with the surface elevations at Godia and Okha as input northern and southern boundary at the mouth. Inland boundary at Navlakhi and Kandla were considered to be closed. Four major tidal constituents M2, S2, K1 and O1 (Anonymous, 1930) were used to predict surface elevations at Godia and Okha. Model runs were carried out with Manning number = $30 \text{ m}^{1/3} \text{ s}^{-1}$ and horizontal eddy viscosity coefficient = $0.5 \text{ m}^2 \text{ s}^{-1}$. A time step of 30 seconds was selected which yielded a Courant number of 1.3.

The results obtained from the hydrodynamic model were validated by synchronous current measurements between 3-13 September of 1999 at two locations in the inner and outer regions of the Gulf, and were found to have a good correlation (Fig. 2). We have, therefore, presented depth and time averaged magnitude and direction of currents from the half-hourly results of the simulation studies for HT, LT and MT conditions, which match well with the 2D and 3D modeling results of other studies (Kunte et al., 2005, Vethamony et al., 2005). However, the magnitude of the currents derived from the models was found to be underestimated. Though matches well with the result of models, the direction of the measured currents at two instances have variations of 15-60°

during ebbing-flooding transition of northerly flowing currents at the outer Gulf station.

The Sequential IRS-P4 OCM (Spectral channel central wavelength [bandwidth]: 412[20], 443[20], 490[20], 510[20], 555[20], 670[20], 780[40], 860[40] nm; Spatial resolution: 0.36 km; Payload altitude: 760 km; Recurrent period: 2-days; Satellite overpass: 1200±0020 hrs LST) data for path-09 row-13 for October 1999 - January 2000 (38 scenes) were analysed for synoptic view and supplementing data for field observations because the imageries of September 1999 were mostly not cloud free due to prevalent southwest monsoon. The algorithm initially proposed by Tassan (1994), and later modified in-house for the OCM-processing software and SeaDAS (SeaWiFS Data Analyses Software; SAC Report, 2004) has been utilized. The suspended sediment concentrations (TSM) have been derived using water-leaving radiance in band 490, 555 and 670 nm using the following relations:

$$\text{Log}(S) = 1.83 + 1.26 \text{Log}(X_s) \quad \forall \quad 0.0 \leq S \leq 40.0 \text{ -----(1)}$$

where S is suspended sediment concentration in mg l^{-1} and X_s is variable defined as:

$$X_s = [Rrs(555) + Rrs(670)] \times \left[\frac{Rrs(555)}{Rrs(490)} \right]^{0.5} \text{ -----(2)}$$

where $Rrs(\lambda)$ is remote sensing reflectance in respective wavelengths (λ). The retrieval accuracy of SSC from OCM data is $\pm 15\%$ (SAC Report, 2004).

3.0 Results

The depth and time averaged maps of simulated current vectors during low, high and mid tide conditions for the month of September of 1999 together with measured TSM (at 26 stations) during these tidal phases are presented in Figs. 3-5. The hydrography, as expected, is dynamic in response to the propagation of tide. The magnitude of the currents progressively increases from 68-125 cm s⁻¹ (at mouth) to 125 -185 cm s⁻¹ in the inland region of the bay. The direction of the currents also varies. From strong, alongshore component at the mouth, the flows move in (out) during flood (ebb) with stronger across shelf component in the central bay (Figs. 3-5). Synchronous in situ TSM maps suggest that the Gulf waters generally have high TSM (between 21-69 mg l⁻¹), and have a trend that decreases inland. We also observed a large variation in TSM during different tidal phases. All the stations have variable response to the tide. Broadly, the inland region of the Gulf has uniformly least TSM during all the tidal phases. The middle portion of Gulf, by and large, has reduced TSM during mid tide, though it is more turbid compared to the inner Gulf. The outer Gulf, which has the highest TSM, however, has different trends along the two flanks. The entire northern region is found to have higher TSM compared to the southern region during all the tidal phases (Figs. 3-5).

The clay minerals show high spatial variability (Fig. 6). Illite is the most dominant clay species followed by chlorite, kaolinite and smectite. Illite and chlorite show inland reducing trend along the northern flanks of the Gulf. Kaolinite and smectite are deficient in the sediments at the mouth all along the northern region. The clays in the sediments of the shelf and in the rivers were

also highly variable (Fig. 7). On the shelf, sediments were enriched in illite and chlorite (Fig. 7 a-b). The sediments from the Rivers Aji and Machchu have high smectite with minor illite and kaolinite (Fig. 7 c-d).

4.0 Discussions

The Gulf of Katchchh lies in a semi-arid region, with only 50 cm annual rainfall. The rivers in the regions are short and estuarine with insignificant discharge (Table 1). Because of high measured amount of TSM ($21-69 \text{ mg l}^{-1}$), the Gulf waters may be termed turbid, and the magnitude of turbidity diminishes inland. Kunte et al. (2003) have determined TSM from satellite data, which is grossly underestimated (maximum $< 4 \text{ mg l}^{-1}$) with respect to the measured TSM. This may be related to the algorithm used in this study, which may not be suitable for case II waters of the Gulf. Despite the insignificant fluvial input, existence of turbid water in the entire Gulf is rather intriguing. There is no reports of higher aeolian contribution into the region to sustain such a high TSM. The sediment flux of the local rivers is rather low (Table 1), and even if the TSM been related with the local fluvial sources, it should have been progressively increasing from the head to the mouth. The zonal distribution of the TSM in the Gulf, therefore, appears not to be related with the local supply. Further, the salinity in the Gulf increases from the mouth to head (Unnikrishnan and Luick, 2003). If the fluvial influx was significant, the inland salinity reduction should have been more pronounced. The salinity trend, therefore, further corroborates a reduced local fluvial influence in the Gulf. This implies that, to a larger extent, the influx of the sediments into the Gulf is not contributed from

the local rivers. The other source of these sediments may be from re-suspension due to large tidal currents. The sub-bottom physiography of the outer Gulf is even, with a deposition of about 18 m thick sediments with no scouring marks (Chauhan and Vora, 1990), and therefore, the re-suspension or scouring from the seabed appears not to be the process that contributes significantly to the TSM load of the surficial waters. Further, because the currents are stronger inland, the intensity of the scouring should have been more intense with high TSM in shallower waters in the interior regions. The TSM maps, however, have contradictory trends, and therefore, do not support significant contribution either through scouring or from local fluvial sources.

Contiguous to the highly turbid waters located along the northern flank at the mouth, the offshore stations of the present study have higher TSM (Figs. 3-5). We have evaluated regional TSM distribution from the Ocean Color Monitor (OCM P-4) imageries from this region (Fig. 8), and that of Kunte et al. (2003). All along the entire northern region between the study area and the mouth of River Indus located about 100 km north, the coastal waters are highly turbid (Fig. 8), though quantum of turbidity in the imageries are specifically less compared to in situ measurements. During the SW monsoon, the hydrography being alongshore (Shetye et al., 1990) is favorable for the dispersal of flux of the Indus into this region, which has peak discharge during this time. It is inferred, therefore, that the terrigenous flux of the Indus is transported along shelf by the SW monsoon hydrography as reflected in the high TSM of the offshore stations. Chauhan (1994) has found higher deposition of the clays of

the Indus on the inner shelf region of the Gulf. Such inference is further corroborated by the accretionary physiography on the entire shelf between the mouths of the Indus and the Gulf (Chauhan et al., 2000). Cattaneo et al. (2003) have reported shore parallel advection of the terrigenous flux during late Holocene along Adriatic shelf, and support our thesis of advection of large terrigenous flux by the shelf hydrography contributing to the accretionary physiography in this region.

The macrotidal hydrography of the Gulf appears to play a specific role for the inland advection of the offshore turbid waters. The currents are alongshore and move in (out) during flood (ebb) tide, and become stronger inland with amplification of tide ($>68 - 125 \text{ cm s}^{-1}$ at the mouth; $125-185 \text{ cm s}^{-1}$ in the inner Gulf). Semi-diurnal ebb and flood tidal phases are not synchronous at the mouth and at the head. Initiation of flood phase at Okha (at the mouth) is found to be timed with the ebb at Navalaki (inland Gulf; Pradhan et al., 2004), which implies that currents flow in opposite direction in the inner and outer Gulf during initial stage of flooding at Okha (Fig. 4). This specific hydrography appears to be crucial and specific. The high magnitude flood flows draw the TSM rich offshore turbid waters inland into the Gulf along the northern flank and advect and distribute TSM into the inner regions of the Gulf. An asynchronous ebb-flood flow of the inner - outer regions and large variations in tide regulated currents and water levels at the different regions of the Gulf (Figs. 3-5); lead to the formation of residual eddy currents (Vethamony et al., 2005). These eddies appear to restrict inland advection of suspended matter.

Gao et al., (1990) have also found sorting of sediments by the stronger ebb currents in the Xiangshan Bay, which further corroborates the role of tidal forcing on sediment dispersal pathways.

The clay minerals are $< 2\mu\text{m}$ in size, and have potential to be carried in suspension for considerable distance in the open ocean, though these are liable to be flocculated in an estuarine environment dominated by the mixing of saline – fresh waters. Each individual clay mineral, being produced from specific geology and climate of any given region, is considered source specific (Biscaye, 1965; Weaver, 1989). The inner Gulf is highly saline for there is no significant fluvial influx due to prevalent climate, and therefore there is not much large scale mixing of the waters of different salinity to support flocculation of clays from the local sources. The clay minerals in the suspended matter from the study area are evaluated, therefore, to decipher the sources of the sediments. The Gulf has illite and chlorite as predominant clays. Smectite and kaolinite are also present (Fig. 6) as minor clays. Local geology being predominantly basalt with Cretaceous sedimentary rocks (Krishnan, 1968), smectite is the clay expected to be contributed from the local sources. In order to determine the clays contributed from the local sources, two samples from the Rivers Aji and Machchu were analyzed. The clays in the load of these rivers are smectite, kaolinite and illite (Fig. 7 c-d). However, we have observed chlorite in all the samples, with a decreasing inland trend in the Gulf waters. Chlorite is the specific clay mostly produced in the arid, cold climate, (Weaver, 1989), and not in semi-arid, hot climate which is prevalent in the hinterland of

the Gulf. Due to this prevalent climate, it is not produced locally and is absent in the local rivers. The source of this clay therefore, appears non-local. We have evaluated available data also on the clays in the load of the River Indus (Konta, 1985). Illite, chlorite with minor kaolinite are the clays present in the order of abundance in this river (Konta, 1985; Table 1). The presence of chlorite in the Indus appears related to its catchment area, which mostly lies in the Himalayas with the arid, cold climate. The sediment samples from the inner shelf between the mouth of Indus and Gulf (Fig. 1) show dominant chlorite and illite assemblage (Fig. 7, a-b; Chauhan, 1994). These clays have high contents all along the northern flanks with inland reducing trend (Fig. 6). This may be interpreted as along-shore advection of the influx of the Indus. Kaolinite and smectite are, however, enriched along the southern flank and in the inner region of the Gulf. The specific distribution trend of illite and chlorite (which is not observed in the load of local rivers), together with distribution trend of local clays therefore provides additional support to our thesis of influx of sediments of the Indus into the inland regions of the Gulf.

It is therefore concluded that the highly turbid waters of the Gulf are due to inland influx of the sediments of the Indus by the specific macrotidal hydrography of this region. The results also signifies the role of distal fluvial sources over considerable inland regions, here to before unknown, along the entire 7500 km long coast of India. The 18 m thick deposition in the Gulf during Holocene is further manifestation of large-scale movement of terrigenous flux of

Indus into the Gulf by the tidal currents after the submergence of the Gulf associated with changes in sea level since 10 Ka BP.

Such inland influx of sediments has implications: (i) For estimating the flux of rivers from time series trap experiments, or in palaeoclimatic reconstruction from cores that have linearly correlated terrigenous flux with the discharge magnitude of the Indus, although such flux also advects and sinks inland, and not accounted in these estimations (Nair et al., 1989; Van Rad et al., 1999), and (ii) for hydrographic regulated dispersal processes vis-à-vis turbidity, crucial for sustaining coral and mangrove ecosystems abundantly found in this region, and influencing regional productivity and CO₂ fluxes regulating carbon sink.

Acknowledgement:

The authors are thankful to the Director NIO for providing the facilities. We thank Commanders S. Raguvanshi, J. Dhayya, D. Singh of Indian Navy/Coast Guard for help in the collection of water samples and logistic support. We thanks editor in chief, Nathalie Fagel and an anonymous referee for constructive review and suggestions for the improvements to the manuscript.

NIO contribution no 4075.

References:

Anonymous, 1930. Tides and harmonic constants. Special Publication No. 26.

International Hydrographic Bureau, Monaco.

Abbott, M. B., Damsgaard, A., Rodenhuis, G. S., 1973. System 21, Jupiter, A Design System for Two-Dimensional Nearly Horizontal Flows, J. Hydraulic Res. 1, 1-28.

Abbott, M. B., 1979. Computational Hydraulics – Elements of the Theory of Free Surface Flows, Pitman Publishing limited, London. pp. 324.

Biscaye, P. E., 1965. Mineralogy and sedimentation in the recent deep-sea clay in the Atlantic and adjacent seas and oceans. Bull. Geol. Society Ame. 76, 803-832.

Carroll, D., 1970. Clay mineral a Guide to their X-ray identification. Geological Society of America, Colorado. pp. 80.

Cattaneo, A., Correggiari, A., Langone, L., Trincardi, F., 2003. The late Holocene Gargano sub-aqueous delta, Adriatic shelf: Sediment pathways and supply fluctuations. Mar Geol. 193, 61-91.

Chauhan, O.S., Vora, K.H., 1990. Reflection seismic studies in the macrotidal Gulf of Kachchh, India: evidences of physiographic evolution. Continental Shelf Res. 10, 385-396.

Chauhan, O.S., 1994. Influence of macrotidal environment on shelf sedimentation, Gulf of Kachchh, India. Continental Shelf Res. 14, 1477-1493.

Chauhan, O.S., Almeida, F., Suneethi, J., 2000. Influence of sedimentation on the geomorphology of the northwestern continental margin of India, Mar. Geodesy 23, 259-265.

Gao, S., Xie, Q.C., Feng, Y.J., 1991. Fine-grained Sediment Transport and Sorting by Tidal Exchange in Xiangshan bay, Zhejiang, China. *Estuarine. Coast. Shelf Sci.* 31,397-409.

Konta, J., 1985. Mineralogy and chemical maturity of suspended matter in major river sampled under the SCOPE/UNEP project. In: *Transport of carbon and minerals in major world river Part III*, Digen, T. Kempe, S (Eds), *Mitteilunga aus dem Geologisch-Palantologischen Institut der Universität Hamburg*, pp. 569-592.

Krishnan, M.S., 1968. *Geology of India and Burma*. Higginbotham (P) Limited, Madras, pp.536.

Kunte, P.D., Wagle, B.G., Sugimori, Y., 2003. Sediment transport and depth variation study of the Gulf of Kutch using remote sensing, *Int. J. Remote Sens.* 24(11), 2253-2263.

Kunte, P.D.; Zhao, C.; Osawa, T.; Sugimori, Y., 2005. Sediment distribution study in the Gulf of Kachchh, India, from 3D hydrodynamic model simulation and satellite data. *J. Mar. Syst* 55, 139-153.

Milliman, J. D., Meade, R. H., 1983. World wide delivery of river sediment to the oceans. *J. Geol.* 91, 1-21.

Nair, R.R., Hashimi N.H., Rao, P.C., 1982. Distribution and dispersal of clay minerals on the western continental shelf of India. *Mar. Geol.* 50, M1 M9.

Nair, R.R., Ittekkot, V., Manganini, S.J., Ramaswamy, V., Haake, B., Degens, E.T., Desai, B.N., Honjo, S., 1989 Increased particle flux to the deep ocean related to monsoons. *Nature* 338, 749-751.

Nigam, R., Hashimi, N.H., Menezes, E.T. Wagh, A.B., 1992. Fluctuation in sea level off Bombay (India) between 14,500 to 10,000 years Before Present Curr. Sci., 63, 309-311.

Pradhan, Y., Rajawat, A.S., Nayak, S.R., 2004. Application of IRS-P4 OCM data to study the impact of tidal propagation on sediment dynamics in the Gulf of Kachchh. Indian J. Mar. Sci. 34, 157-163.

SAC Report, 2004 Atmospheric Corrections, Bio-optical algorithm development and validation of IRS-P4 OCM data (IRS-P4 OCM Utilisation/SATCORE Project Report). Scientific Report No. SATCORE/SAC/RESA/MWRG/SC/ 01/02, pp 98.

Sharma, H.R., Devasahayam, R., 1985. Tidal behaviour of Gulf of Kachchh. In: 52nd Annual R&D Session CBIP (Aurangabad), pp. 33-44.

Shetye, S.R., Gouveia, A.D., Shenoi, S.S.C., Sunder, D., Michael, G.S., Almeida, A.M., Santanam, K., 1990. Hydrography and circulation off the west coast of India during the southwest monsoon 1987. J. Mar. Res. 48, 359-378.

Tassan, S., 1994 Local algorithm using SeaWiFS data for retrieval of phytoplankton pigment, suspended sediments and yellow substance in coastal waters. Appli. Optics 12, 2369-2378.

Unnikrishnan, A.S., Luick, J.L., 2003. A finite element simulation of tidal circulation on the Gulf of Kutch. India. Estuarine. Coast. Shelf Sci. 56, 131-138.

Vethamony, P., Reddy, G.S., Babu, M.T., Desa, E., Sudheesh, K., 2005. Tidal eddies in a semi-enclosed basin: a model study. Mar. Env. Res. 59, 519-532.

von Rad, U., Schaaf, M., Michels, K.H., Schulz, H., Berger, W.H., Sirocoko, F., 1999. A 5000 – year record of climate change in varved sediments from the

oxygen minimum zone off Pakistan (northeastern Arabian Sea). *Quat. Res.* 51, 39-53.

Weaver, C.E., 1989. *Clays, Muds and Shales*. Elsevier, Amsterdam, pp. 819.

Table 1. Characteristics of the fluvial sources in the Gulf of Kachchh during the peak discharge (modified from Nair et al., 1982; Sharma and Devasahayan, 1985; Hasan Masoor (www.himalmag.com/2002/july/report_4.htm)). Refer Fig. 1 for the location of the rivers. Star denotes relative abundance of each clay in the load as given in Konta (1985). For the location of shelf (A and B) and rivers sampling stations (C and D) for clay analysis, refer Fig. 1.

Name of the River/ sample Id for clay station	Discharge ($\text{m}^3 \text{s}^{-1}$)	Sediment Flux (g l^{-1})	Clays in the load			
			I	C	K	S
Adhoi	2.1	0.11 – 2.15				
Sakara	4.0	0.04 – 0.27				
Jhinhoda	1.0	0.14 – 2.5				
Phuldi	24.0	0.14 – 0.95				
Machchu (D)	476.0	0.20 – 1.99	*		**	****
Demi	438.0	0.90 – 2.65				
Aji (C)	3226.0	0.29 – 2.26	*		**	****
Indus\$	175×10^9	200×10^6 Tons	****	**	*	
Shelf sample A (Northern shelf)	—	—	****	***	*	*
Shelf sample B (Southern shelf)	—	—	****	**	*	**

\$ annual discharge rates; I=illite, C=chlorite, K=kaolinite, S=smectite

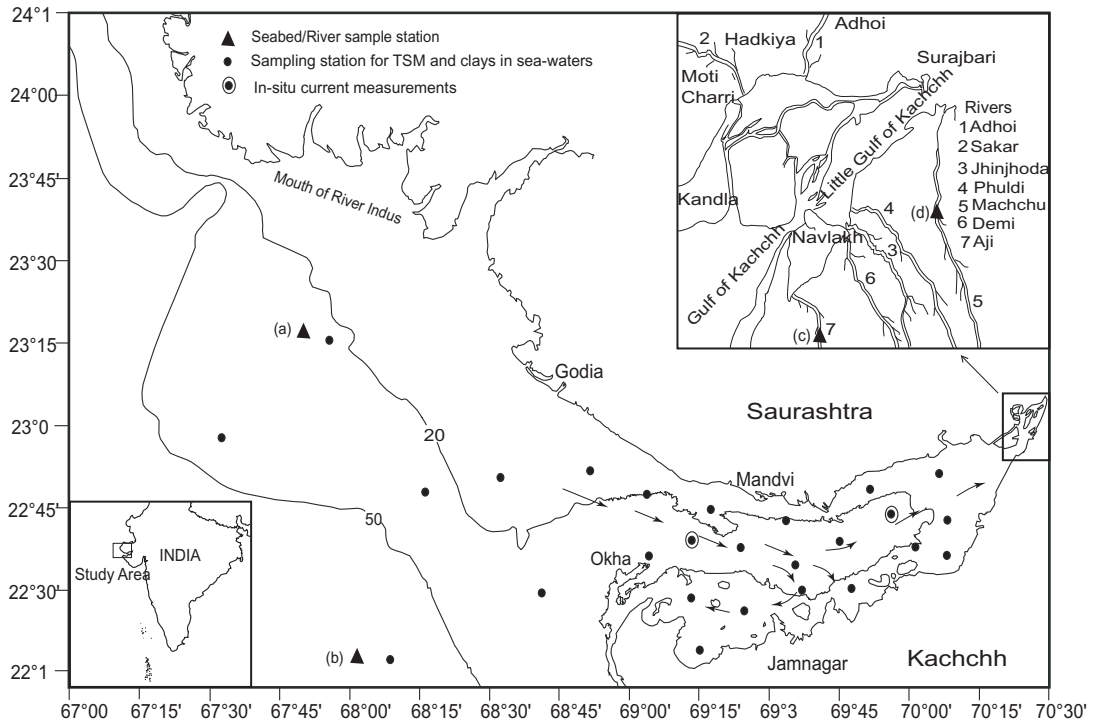


Fig. 1. The study area with location of stations for synchronous TSM and current measurements. Locations where insitu synchronous currents measurements for model validation has been carried out are circled. The triangle represents the locations of stations for clays analysis from the shelf and Rivers Aji and Machchu. The advection of the influx of River Indus is also schematically shown.

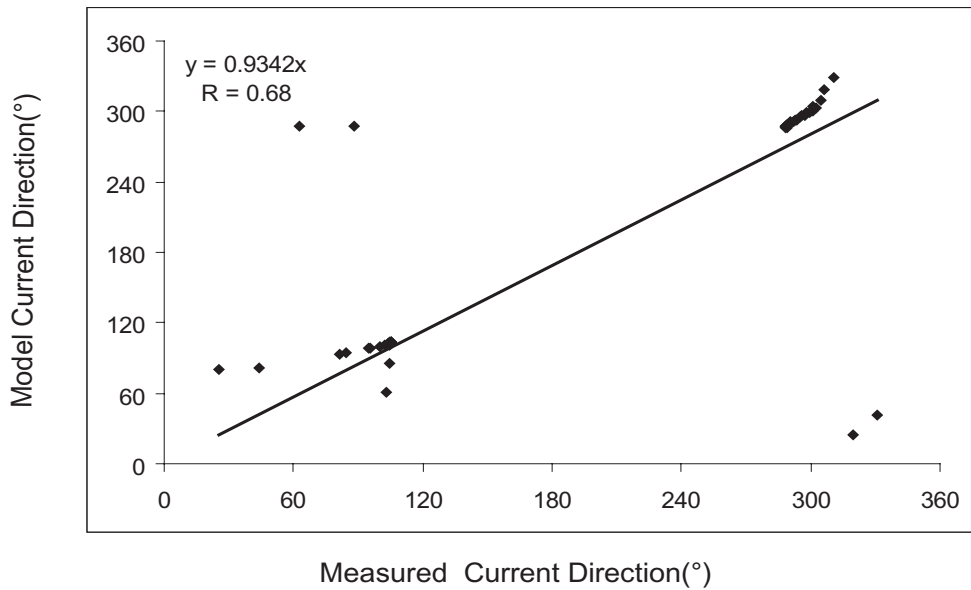
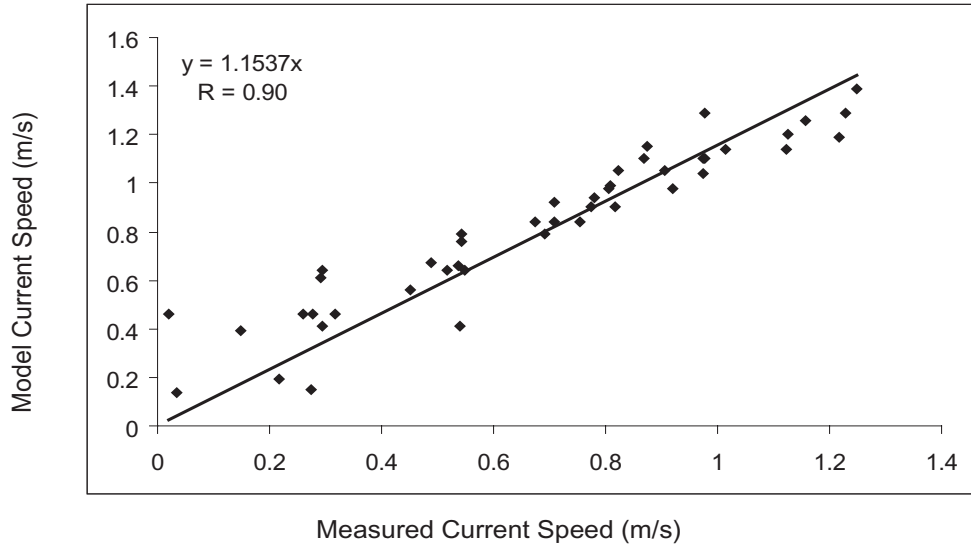


Fig. 2. Comparisons of measured in situ (between 3-13 September 1999) and model current vectors at two locations. Refer Fig. 1 for the locations of the stations.

Fig 3

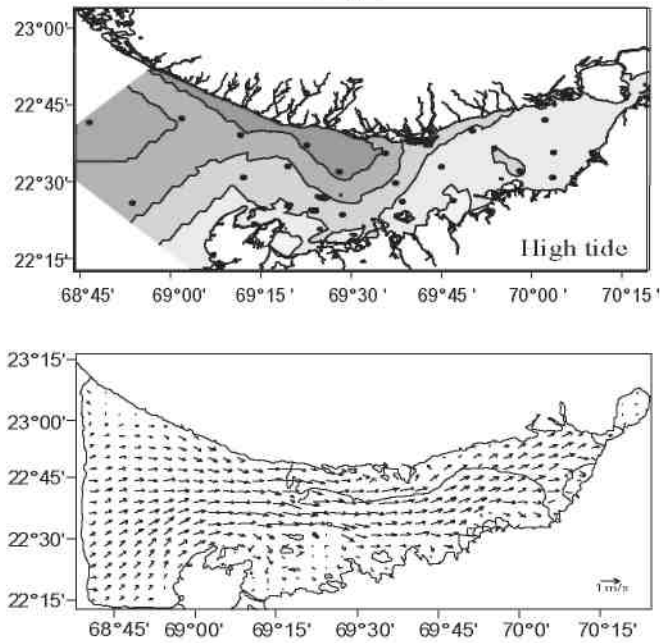


Fig. 3. Current vectors and TSM (mg l^{-1}) during high tides deduced from hydrodynamic modeling and filter residue.

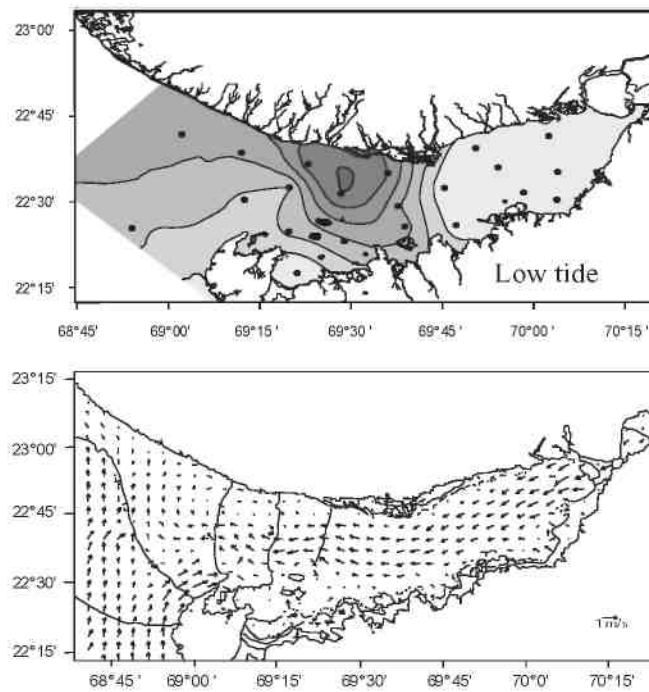


Fig. 4. Current vectors and TSM (mg l^{-1}) during low tides deduced from hydrodynamic modeling and filter residue.

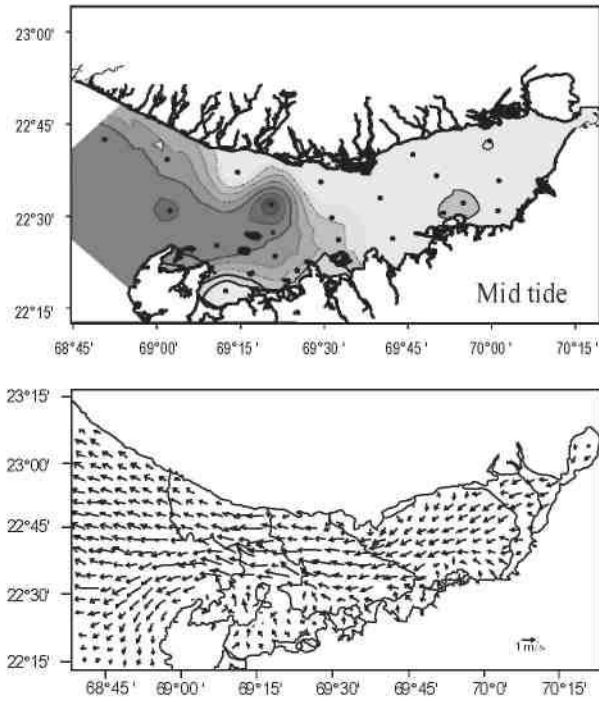


Fig. 5. Current vectors and TSM (mg l^{-1}) during random tides deduced from hydrodynamic modeling and filter residue.

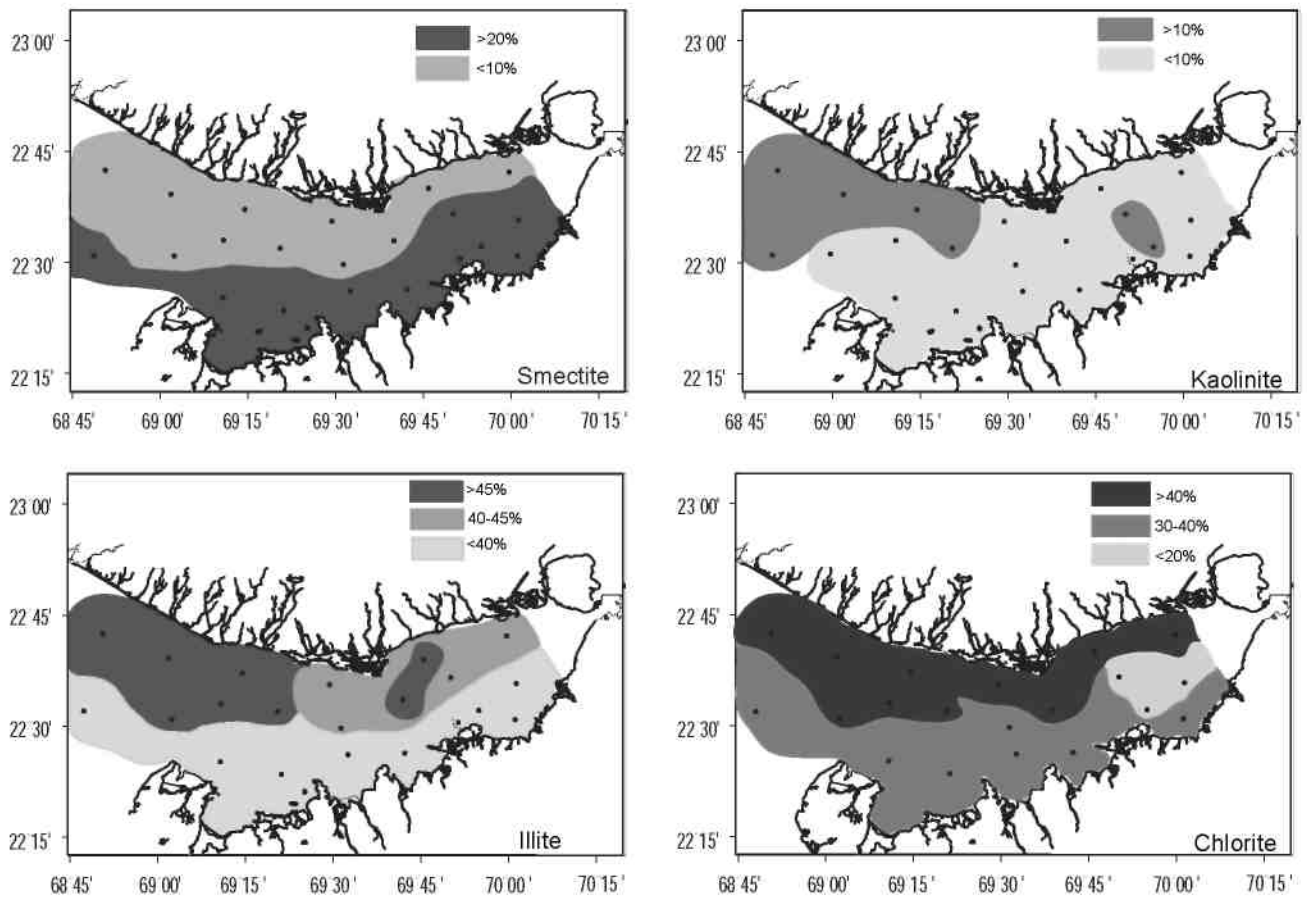


Fig. 6 Spatial distribution of chlorite, illite, kaolinite and smectite in the Gulf waters.

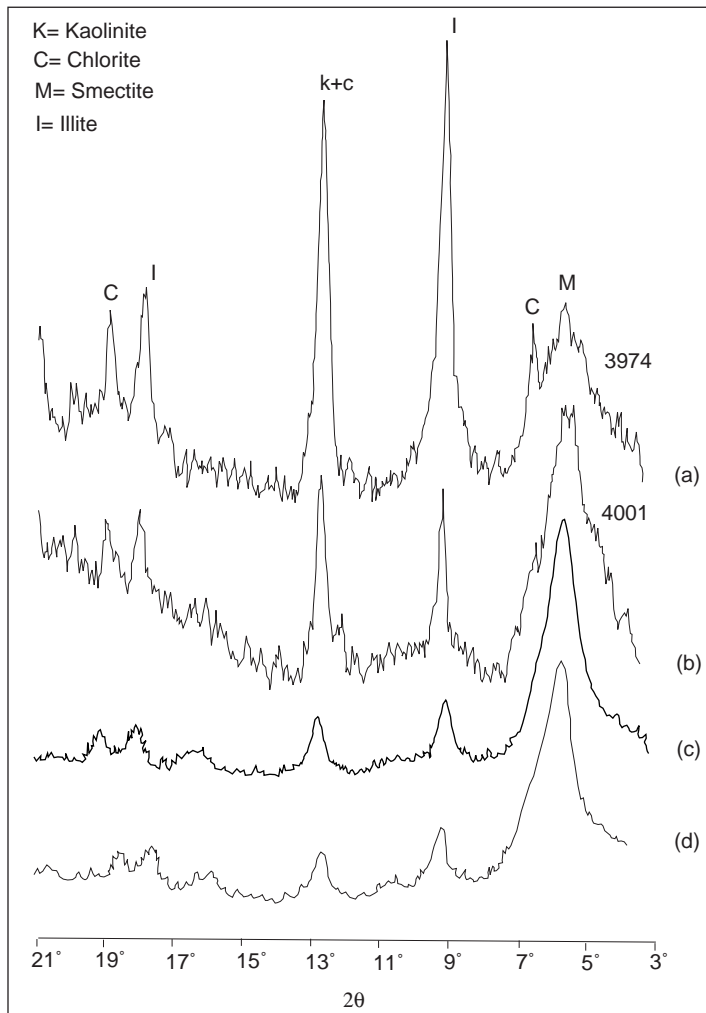


Fig. 7. Glycolated X-ray diffractogram of selected seabed samples from the inner shelf (A-B) and from the Rivers Aji (C) and Machchu (D). Inset shows locations of rivers and their sampling stations in Fig. 1. For location of the samples A-B, also refer Fig. 1. (I=illite, C=chlorite, S=smectite, K=kaolinite)

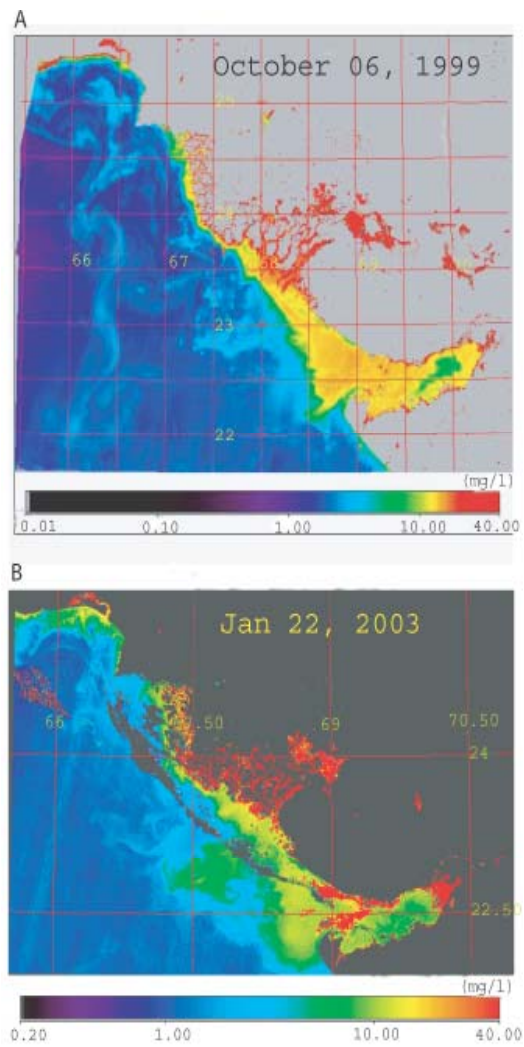


Fig. 8. OCM P-4 imageries of the Gulf of Kachchh during LT (A) and HT (B).